

Studies of the Consequences of Carbon Sequestration Using Los Alamos Ocean Models

Shaoping Chu^a, Scott Elliott^a, Mathew Maltrud^b, Fei Chai^c and Francisco Chavez^d

^a Los Alamos National Laboratory, Mail Stop D401, Los Alamos, NM 87545

^b Los Alamos National Laboratory, Mail Stop B216, Los Alamos, NM 87545

^c University of Maine, School of Marine Sciences, 5741 Libby Hall, Orono, ME 04469

^d Monterey Bay Aquarium Research Institute, 7700 Sandholdt Road, Moss Landing, CA 95039

Abstract

A fine resolution marine biogeochemistry model has been developed in the context of the global Parallel Ocean Program. Iron and carbon cycling are included along with macronutrient chemistry and multiple plant species ecodynamics. The biogeochemical OGCM is here applied to study efficiency and effects for dozens of simulated mixed layer trace metal enrichments, configured at close to the IronEx scale and distributed throughout the major HNLC zones. Test introductions south of New Zealand indicated early on that bloom behaviors and filamentation documented by satellite ocean color instruments would be well captured. Across a global suite of thirty iron patches each one hundred kilometers on a side, plant nitrogen content typically reached several micromolar over a month of processing. Flow of carbon from the background inorganic pool into living and detrital forms was computed for the simulated enrichments and compared with results from recent in situ experiments. Agreement was close for all forms except the zooplankton. Patches were ranked together according to net export. Equatorial introductions proved most effective because warmer waters stimulate the overall ecology. At high Southern latitudes and in the Gulf of Alaska biogeochemistry developed more slowly. Several of the model area export values agreed closely with the results of IronEx type work. Evolving minima in carbon dioxide partial pressure dramatize engineering aspects of the localized metal injections. It is noted that secondary effects on trace gases such as dimethyl sulfide will be of interest and that the biogeochemical OGCM is already equipped with the appropriate processing channels. Injections of inert material representing CO₂ were made into the program deep sea in preparation for the study of effects on the abyssal carbonate system. Return to the surface occurred most rapidly beneath the convectively active waters of the circumpolar current.

Introduction

Marine carbon management options are currently garnering close consideration by the scientific and policy communities (IPCC 1996 and 2001). Among the strategies available, introduction of micronutrient iron into the mixed layer has received the majority of field work attention. In situ enrichments of increasing size have occurred with increasing frequency (Chavez et al. 2003). The iron patches have been, and in the foreseeable future will continue to be, deployed at the physical oceanographic submesoscale (3 to 30 kilometers in horizontal dimension). Regional level injections occur naturally on a seasonal and interannual basis, since the metal is supplied chiefly by winds (Fung et al. 2000). Engineered equivalents have already been simulated in biogeochemical OGCM codes (Sarmiento and Orr, 1991) and may someday demand policy assessment. However, underlying inputs of macronutrient nitrate will remain eddy driven over large areas (McGillicuddy et al. 2003; Elliott and Chu 2003). Details of the carbon cycle efficiencies and biogeochemical effects for trace metal injection must thus be simulated in turbulence resolving transport frameworks, to ensure accuracy and validate any coarser production computations.

We have been involved over the last few years in development of a fine mesh biogeochemical simulator (e.g. Chu et al. 2003) suitable to the study of iron enrichment over the full range of High Nutrient Low Chlorophyll waters (HNLC; Watson and Liss 1998). Multiple elemental cycles have been sequentially incorporated into eddy resolving versions of the global Parallel Ocean Program (POP; Maltrud et al. 1998). The geochemical processing is controlled by multiple plant species/trophic level ecodynamics. In the present work we describe application of the biogeochemical OGCM to manifold simulated iron patch additions. The introductions are made at scales approaching those in real in situ experiments of the past decade (e.g. Martin et al. 1994; Coale et al. 1996; Boyd et al. 2000), but maintaining several mesh points in the horizontal such that filamentation can be represented.

Our text opens with a brief description of construction and validation of the biogeochemical POP model. Preliminary (three patch) tests and global statistical experiments are then accounted in terms of evolving patch morphology, as well as integrated flow of carbon through trophic levels and detrital forms. Geographic areas studied are ranked in terms of their export potential. For many key parameters including phytoplankton densities, particulate organic concentrations and vertical fluxes, comparisons with measurements are encouraging. A major exception is constituted by the ecological grazing bins. We speculate that a distinction of micro- from mesozooplankton will ultimately allow modulation of both plant and grazer densities. Carbon dioxide partial pressure fields are displayed with engineered, eddy sculpted minima highlighted. We note that our global biogeochemistry coding embraces production/removal by the geocycling system for trace volatiles of atmospheric chemical interest (Chu et al. 2001). Several authors have noted that these will be generated as byproducts of engineered blooms (e.g. Elliott and Chu, 2003). A set of deep tracer releases has also been performed, in anticipation of the need to investigate influences of abyssal sequestration on the carbonate system. Return rates are listed for the major basins at a one hundred year time horizon.

The Model

The Parallel Ocean Program or POP is a Fortran updated descendant of the Bryan Cox Semtner Chervin family of OGCM codes (Semtner, 1986). Gridding is normally Cartesian in the vertical and numerics are based on the primitive equations. POP has been developed over the last decade at Los Alamos National Laboratory on a sequence of supercomputers supplied first by Thinking Machines (the Connection Machines 2 to 5), then Cray (in particular the T3D), and finally Silicon Graphics (the most recent platforms have been the Origins 2000 and 3000). Typically 100 to 1000 processors have been dedicated to circulation problems such that basin and global scale resolutions down to one tenth degree could be achieved. Validation of physical oceanographic parameters has been conducted against satellite sea surface height determinations and characterizations of Sverdrup flow in major current systems. Improvements which have accrued in the model physics/computations include incorporation of a nonrigid oceanic lid (surface), stretched meshes with shifted poles avoiding the familiar Mercator singularity, partial bottom cells, geodesic gridding, and hybrid isopycnal layering in the deep sea. The sequence of publications Dukowicz et al. (1993), Maltrud et al. (1998) and Smith et al. (2000) may be consulted for further details.

Biogeochemistry has entered the POP frameworks in stages beginning with a nitrogen cycle sufficient to represent chlorophyll distributions in nonHNLC areas (Fasham et al. 1990; Fasham et al. 1993; Sarmiento et al. 1993; Ryabchenko et al. 1997). Iron cycling has been included more recently, following the NCAR example with regard to mechanism (Moore et al. 2002) and employing atmospheric chemistry-transport derived dust inputs (Fung et al. 2000). Silicon processing is now incorporated such that the diatoms may be represented as bloom dominating organisms (Chai et al. 2002). Carbon cycling and carbonate acid base chemistry are OCMIP consistent but derive largely from Broecker and Peng (1982) and follow ons (Bacastow and Maier-Reimer 1990). The coccolithophorids are treated as a temperature dependent fraction of the nondiatoms, with effects included for calcium carbonate hard part formation on alkalinity (Maier-Reimer 1993). The model lower boundary is currently set at 200 meters based on standard biogeochemical climatologies (Broecker et al. 1982; Levitus et al. 1993; Conkright et al. 1998; Doney et al. 2002). Runs take physical initial conditions and temperature/salinity fields from pure POP computations. Generally the biogeochemistry calculations begin in the middle 1990s and come to global biological steady state within a few years. Validation has been conducted against the variety of satellite chlorophyll data sets (CZCS and SeaWiFS in particular; Longhurst 1998; Doney 2002) and standard carbon dioxide partial pressure climatologies (Takahashi et al. 2002). The series Chu and Elliott (2001), Chu et al. (2003), Chavez et al. (2003) overviews model construction and validation exercises. Biooptics are broadband but include refraction of PAR at the sea surface, along with absorption and scattering in the Beer's Law sense within the water column. The routines are similar to those described in Sarmiento et al. (1993) and Doney et al. (1996)

Iron Patches

Our iron injection experiments began with the introduction of three 100x100 kilometer patches in the general area of the recent SOFeX experiment (Chavez et al. 2003). The engineered squares were aligned along a meridian just to the east of New Zealand and extending southward almost to the line of maximum sea ice extent. Trace metal concentrations were raised to around one nanomolar, a value corresponding with typical field experiments (see for example the early IronExes –Martin et al. 1994 and Coale et al. 1996). This took place instantaneously over the 10000 square kilometer area and to a depth of 50 meters. The enrichments were made on the first of January in a year during the late 1990s. The date is a simply a round value corresponding with the onset of Southern Hemispheric summer. A sampling of the biogeochemical effects results is offered in Figure 1, at the one month time horizon. Iron distributions show considerable stretching and filamentation, consistent with the influence of mesoscale horizontal turbulence. Bloom zones correspond crudely with the areas of iron maximum. However, biogeochemical waves permeate the chlorophyll structures. The timing of plant maxima across an elongating patch may depend critically on early dilution.

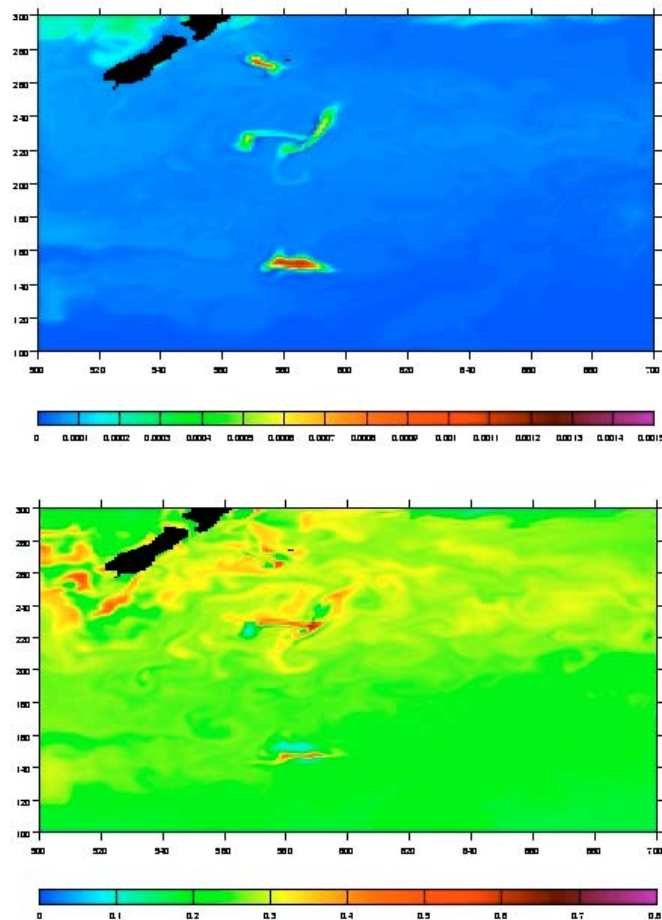


Figure 1. Iron (micromolar) and phytoplanktonic nitrogen (micromolar) in a three patch experiment conducted south of New Zealand, one month into an early summer integration.

A more detailed analysis of POP iron patch behavior has lately been instituted in collaboration with SOFeX mission scientists. Satellite chlorophyll instruments demonstrate that patches which are initially of simple shape (rectangular) soon stretch and twist considerably in the turbulent field (Boyd et al. 2000; Chavez et al. 2003). Inert material clearly displays this tendency as computed by POP and shown in Figure 2. Dispersion should be analogous with that of sulfur hexafluoride in the field because the material is introduced precisely in coordination with the trace metal. Buoy data from SOFeX are also plotted in the figure. Beacons are allocated at several per patch and their positions are provided daily for a six month period. Turbulent dispersion of the patch biogeochemistry should be simulated with fidelity in the POP framework.

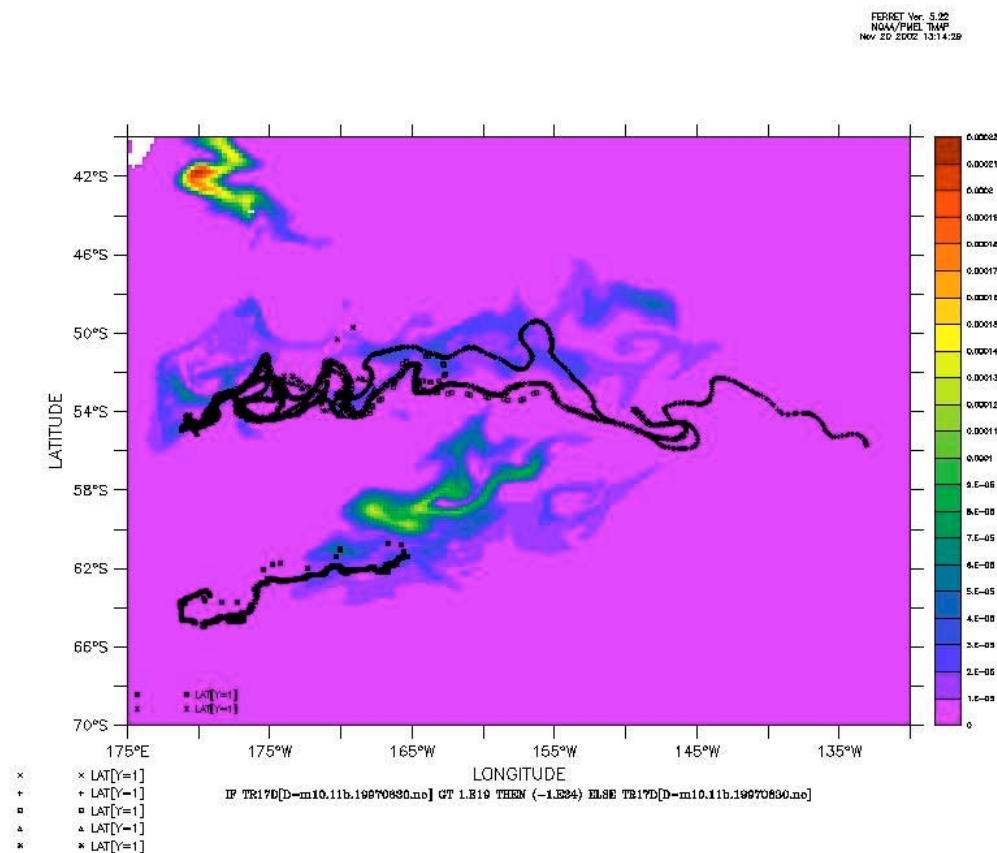
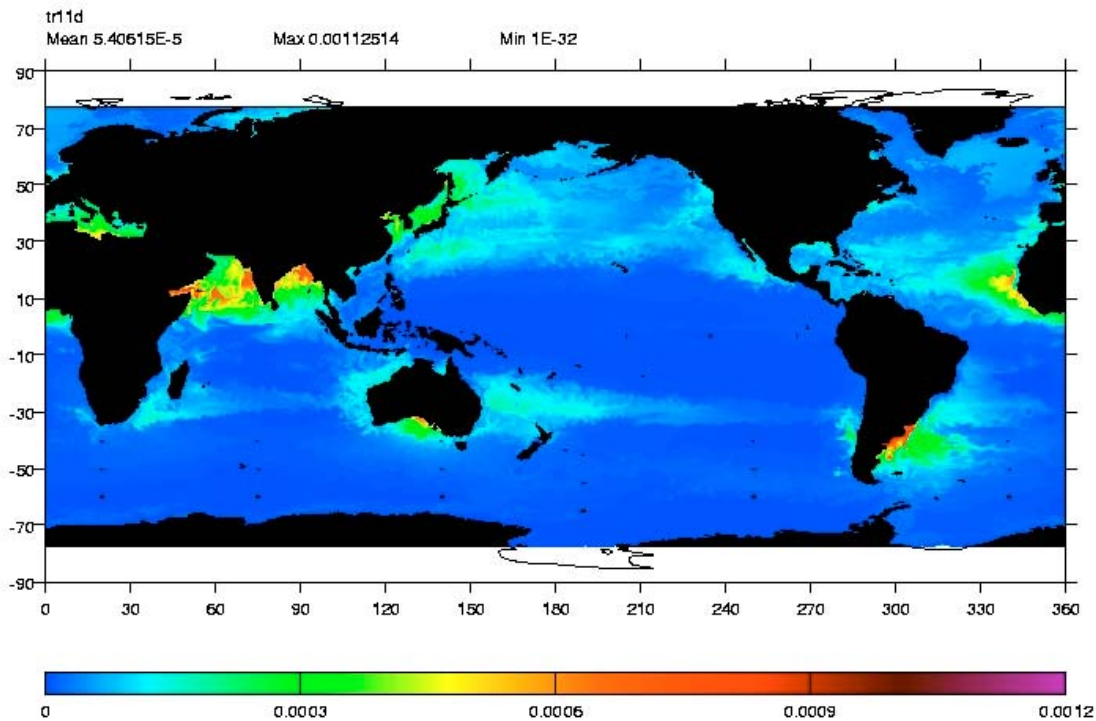


Figure 2. Redistribution of inert material injected into the POP mesh to represent SF6 during a New Zealand three patch run (6 months). SOFeX buoy positions are given for comparison.

As confidence in the preparatory enrichment simulations increased, we moved naturally from the regional scale to a global, statistical approach. Patches were spread evenly through the planetary HNLC regime, limited in number mainly by the requirement that during dispersion they remain segregated over a period of one year. Spacing was determined a priori based on estimates of local horizontal diffusion rates (Bowden, 1975; Tomczak and Godfrey, 1994; Longhurst 1998). Figure 3 indicates the positions and aspects of the sum total of Southern Hemispheric patches, introduced on January 1. A similar density was established in the Northern Hemisphere but six months out of phase (July 1). The simulated Southern Hemispheric iron distribution forms a backdrop to the square enrichment areas. Values are consistent with major measurement studies and models (Johnson 1997; Moore et al. 2002), though the available data are quite sparse.



/am/nearstore1/vol/vol2/ice-bio/spchu/1280_18tracer/bf.set/movies/patch/mfp1.11 b.74461.nc

Figure 3. Global surface concentration distribution for dissolved iron, shown on January 1 with the multiple Southern Hemispheric patch introductions superimposed. Units are micromolar.

Southern and Northern hemispheric phytoplankton distributions are offered in Figures 4 and 5, as they appear twenty days into the run in each case. Response of the POP ecosystem was strong in all equatorial and Southern Ocean locations. Most of the evolving patches reached plant nitrogen maxima of greater than 3 micromolar. Such blooms are consistent with the suite of IronEx results and the now numerous follow ons (Martin et al. 1994; Coale et al. 1996; Boyd et al. 2000; Chavez et al. 2003). Ecosystems utilized the micro- and macronutrients more rapidly at low latitudes. We interpret this as an influence of warm water on growth rates. In the Northern Hemisphere only the Gulf of Alaska shows significant patch activity, in the vicinity of station PAPA. This is of course the area where iron limitation was originally discovered, so that the result is quite reasonable. Some of the largest responses to actual mixed layer metal additions have been observed on the opposite side of the North Pacific, during the Japanese sponsored SEEDS expedition. Phytoplanktonic nitrogen rose to order 20 micromolar, much higher than in any of our simulated locales. A working hypothesis to explain the results hinges on an absence of grazing pressure. POP zooplankton remained active within all the engineered patches.

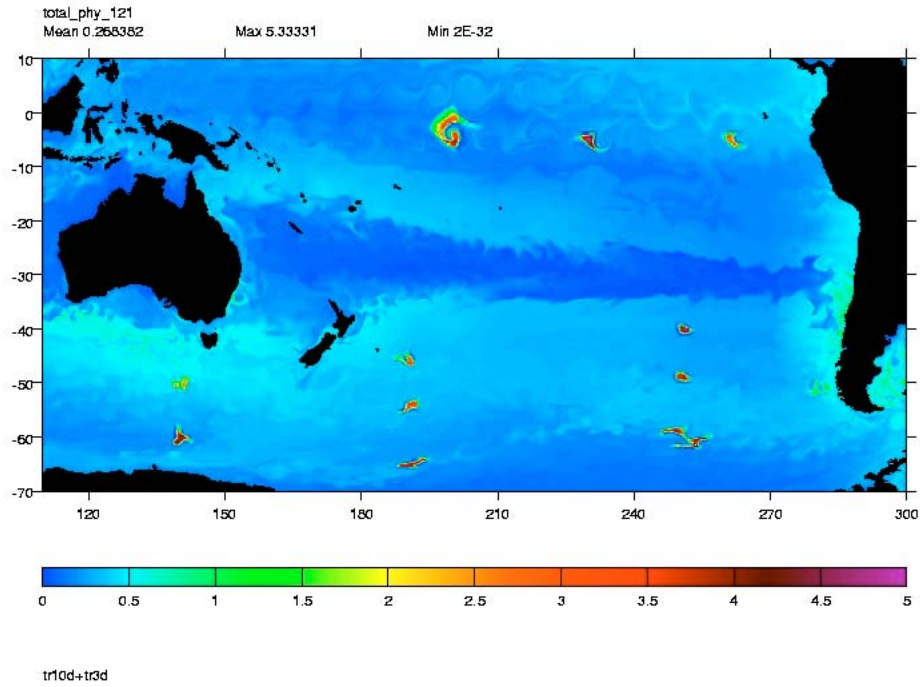


Figure 4. Phytoplanktonic nitrogen distribution (micromolar) twenty days into the run for which iron concentrations are presented in Figure 3.

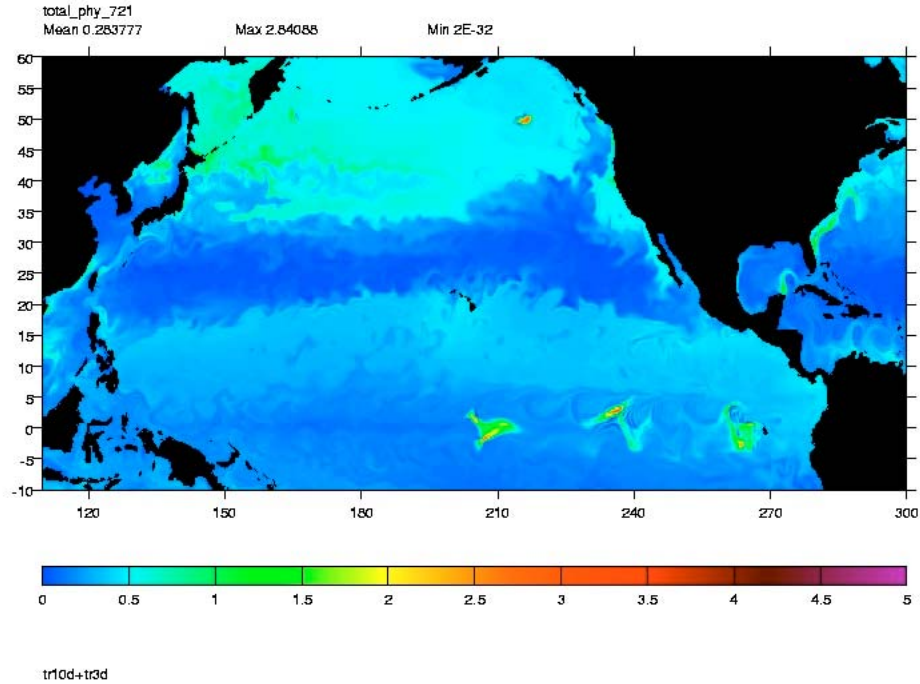


Figure 5. Phytoplanktonic nitrogen distribution (micromolar) twenty days into the Northern Hemispheric simulation corresponding to Figure 4 (patch inception July 1).

The flow of carbon through field-monitored and POP iron ecosystems has been compared in several cases. A summary is offered in Table 1 for one of the relevant calculations. SOFeX point measurements of inorganic and organic chemistry quantities and the components of the biota were averaged over the top thirty meters, corresponding with a normal depth for the summer Southern Hemispheric mixed layer (Tomczak and Godfrey, 1994; Longhurst 1998). Control determinations made outside the patch were subtracted. In order to analyze the analogous biogeochemical POP results, integration routines were developed which were capable of summing mass along the grid, for an arbitrary ecochemical quantity over an arbitrary rectangular area. For shapes (minimally) encompassing the patches, total moles were computed for all major biogeochemical tracers. A difference was then taken relative to a control run with no trace metal additions. Patch volume was derived using the above mixed layer depth and an estimate of area based on iron, chlorophyll or inert tracer thresholds. Particulate organic carbon is here defined to include both living and dead material. A rough conservation is achieved as dissolved inorganic carbon is siphoned into photosynthetic forms, grazed and partially recycled. Considerable carbon is pooled within the mixed layer awaiting export. The model continues to show vertical export of particulate organic carbon several months after fertilization. A major discrepancy between model and measurement occurs in the zooplankton bin. We currently include only a single grazing species in POP ecodynamics. The aggregate consumer is based primarily on the Fasham series of models (e.g. Fasham et al. 1993; Sarmiento et al. 1993). We plan to reconfigure the trophic system soon, such that a mesozooplanktonic species will remove both large plants (bacillariophyceae) and smaller animals. The goal is to modulate overall plant and grazer mass more effectively.

Table 1. The distribution of (Δ) carbon into various inorganic, living and detrital forms near the bloom peak of a Southern Ocean biogeochemical POP iron patch. Sea surface and export fluxes are also provided, in concentration form for a thirty meter mixed layer. SOFeX averages are shown for comparison.

Property (μM)	In situ	Percent DIC	Model	Percent DIC
DIC	-17.3		-21.7	
POC	9	52	10.4	48
Bacteria	1.3	8	3.5	16
Phytoplankton	3.8	22	5.6	26
Micrograzers	0.8	5		
Macrograzers	0	0	5.1	24
Detritus	5.5	32	3.0	14
Export	4.2	24	4.9	22
DOC	5.0	29	0.2	1
Air-sea flux	-1.5	-9	-2.2	-10

Table 2. A ranking of POP iron patches in order of net export at 100 m after 30 days ($\text{mmol C/m}^2/\text{day}$).

155W,3S	206.2117	20W,50S	22.1560
155W,EQ	115.8971	110W,50S	21.5038
125W,EQ	106.0371	20W,60S	19.8867
90W,EQ	70.6826	170W,55S	19.4956
125W,3S	67.5373	170W,65S	19.0325 SOFeX=14.1
95W,3S	42.3180 IronExII=50.0	170W,45S	16.4854
110W,60S	42.2758	140E,50S	15.2340
75E,50S	40.4236	75E,40S	13.1366
75E,60S	30.0988	145W,50N	10.2358
20E,60S	26.8817	20W,40S	4.7734
140E,60S	25.1101	165E,50N	2.1489
20E,50S	24.6124	145W,40N	0.8804
20E,40S	23.5901	140E,40S	0.7113
110W,40S	22.9042	165E,40N	0.2598

Export was computed regularly for all patches and they are ranked at the one month horizon in Table 2. The biological pump was augmented most effectively in the equatorial Pacific. Our interpretation is that blooms proceeded rapidly in warmer waters. Enrichments in the high Southern Ocean drew down less carbon, by perhaps a factor of three to five. Even in summer these waters approach the freezing point. The eastern North Pacific is customarily classified as an HNLC zone but in fact receives substantial annual dust input from Asia. The potential for enrichment to lead to export is curtailed. For several patches situated near some of the actual field work in space/time, measured export rates are provided. Again it would seem that biogeochemical POP is achieving a certain fidelity.

The most dramatic visualization of our simulations for the engineering effects of iron supplementation has come from carbon dioxide partial pressure plots. As DIC is converted into the variety of organic forms, acidity of the manipulated seawater falls. Equilibria in the carbonic acid series shift toward the carbonate ion. Concentrations of the volatile carbon dioxide molecule are suppressed. At the equator it may be the case that the net upward flux is reduced (Broecker and Peng, 1982; Takahashi et al. 2002). At high latitudes the trace gas may be imported. In any case, Figure 6 shows that local perturbations to the partial pressure field may be considerable. Carbon dioxide holes form over the patches, and persist for many weeks.

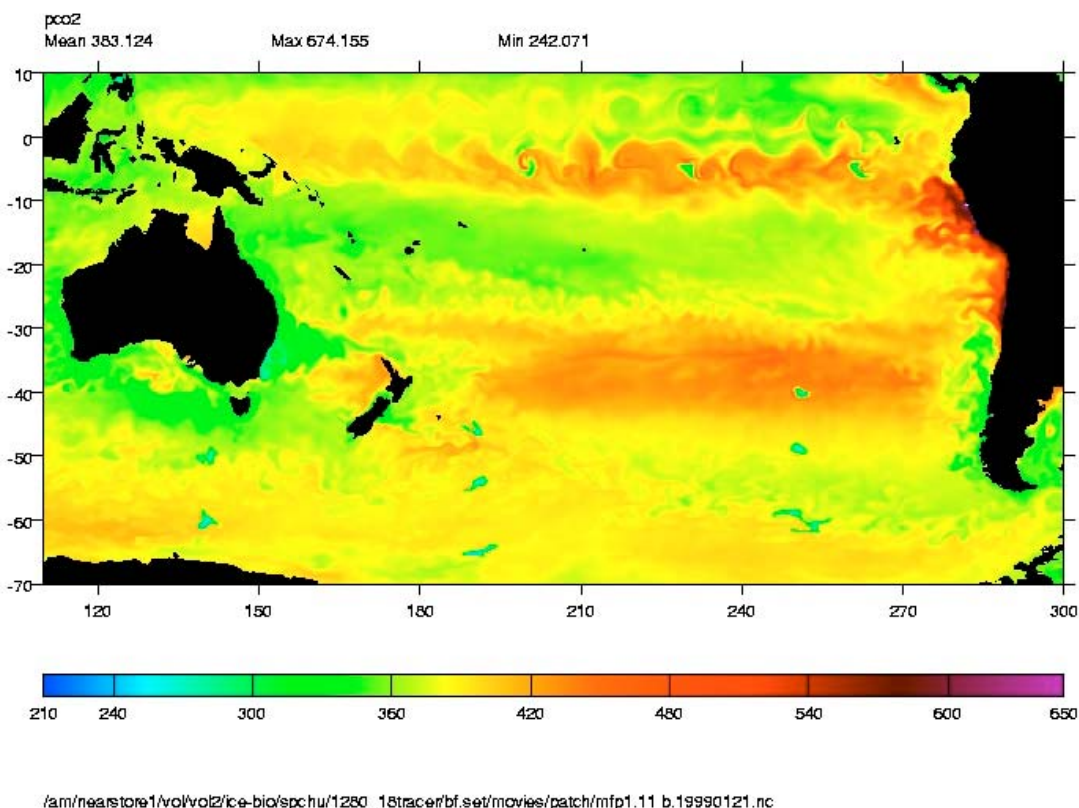


Figure 6. Background and (iron) manipulated carbon dioxide partial pressure fields in the Southern Hemisphere.

Summary and Conclusions

We have applied a fine resolution global model of ocean geochemical processes to simulate the efficacy and outcome for introduction of small iron enrichments, at many locations around the planetary mixed layer. The computed patches filament in a manner consistent with both satellite color imagery of real, IronEx-like blooms and the buoy data forthcoming from deployments/tracking. Plant densities, whether viewed from the perspective of total chlorophyll or nitrogen, are in agreement with measurements made during the major trace metal addition exercises. Conceptual breakdown of carbon conversion into detailed

ecology and detrital categories shows that the model adequately represents production, consumption and export. A ranking of patches initiated in HNLC regions around the globe indicates that temperature strongly influences growth rates and the timing of blooms and export events. Integrated drawdown associated with the model introductions matches values obtained in the field.

As in the case of natural blooms, iron induced production pulses will generate many nonCO₂ trace gases in a byproduct sense. These will include dimethyl sulfide, methyl bromide and other volatile organic species of atmospheric chemical import (Chu and Elliott, 2001; Elliott and Chu, 2003). Some will be exuded directly by phytoplankton, while others will photolyze out of the dissolved organic fraction. Removal may involve bacterial or purely chemical pathways, or both. We have configured biogeochemical POP source and sink terms to include the set of extracarbonate gases. This has been mainly in anticipation of their general earth system significance, but we also intend to revisit numerical iron patch experiments and compute fluxes of the byproduct volatiles into the atmosphere. In background simulations we have achieved solid agreement with trace gas climatologies, as for example in the compilation of Kettle et al. (2001) regarding dimethyl sulfide.

A marine carbon sequestration strategy alternative to iron enrichment will involve direct injection of carbon dioxide into the deep sea (IPCC 1996 and 2001). Phase transitions and hydrate coatings will constitute complicating factors. The overall biogeochemical effects will be controversial because pH and calcium carbonate saturation horizons may be altered at the regional scale. It may be feasible for POP to contribute to assessment studies, along with advanced grid relatives incorporating isopycnal layering below the thermocline and partial bottom cells (accounting more accurately for flow over detailed bathymetry). We are in the process of moving the lower boundary for POP geocycling downward toward the ocean bottom. It will then be possible to apply biogeochemistry coding to CO₂ injection concepts as well as to iron introductions. Preliminary inert tracer experiments have already begun. We have positioned slugs of arbitrary material (representing carbonate or its effects) at several positions upon the ocean floor. Table 3 summarizes results of the runs as return fractions, into the mixed layer after one hundred years of mixing within the general circulation. The POP abyssal tracer computations confirm that injections will be longest lived in the high North Pacific. This portion of the global ocean is known to be noncontributory within the thermohaline overturn. Topography prevents the western boundary currents from transporting saline surface waters far enough toward the pole to enable sinkage. Southern circumpolar waters, by contrast, mix surface to bottom relatively rapidly because deep convection is commonplace.

Table 3. Percentage return of initial mass to surface waters, one hundred years after deep injection in several North Pacific and Southern Ocean locations.

North Pacific gyre	140-150W, 15-25N	1.15E-07
Eastern North Pacific	150-160W, 40-50N	1.74E-06
Western North Pacific	160-170E, 40-50N	4.36E-04
Equatorial Pacific	100-110W, 5S-5N	4.16E-03
Southern Ocean	10-20W, 55-65S	1.51E-02
Southern Ocean	90-100W, 55-65S	7.21E-02
Southern Ocean	90-100E, 55-65S	3.70E-01
Southern Ocean	160-170W, 55-65S	6.64E-01

Acknowledgement This project has been supported by GreenSea Ventures, Los Alamos LDRD (Laboratory Directed Research and Development) and also the U.S. Department of Energy SciDAC project (Scientific Discovery through Advanced Computing, Community Climate System and Earth System Model augmentation grants).

References

Bacastow, R., and Maier-Reimer, E., 1990. Ocean circulation model of the carbon cycle. *Climate Dynamics* 4, 95-125.

- Bowden, K. 1975. Mixing in the global ocean. In *Chemical Oceanography Vol. 1* (Eds. J. Riley and J. Skirrow). Academic Press, New York.
- Boyd, P. W. and 34 others, 2000. A mesoscale phytoplankton bloom in the polar Southern Ocean stimulated by iron fertilization. *Nature* 407, 695-702.
- Broecker, W. S. and Peng, T. H., 1982. *Tracers in the sea*, Eldigio Press, Lamont Doherty Geological Observatory.
- Broecker, W. S., Spencer, D. W., and Craig, H., 1982. GEOSECS Pacific Expedition, Hydrographic Data. U.S. National Science Foundation.
- Chai, F., Dugdale, R. C., Peng, T.H., Wilkerson, F. P., and Barber, R. T., 2002. One dimensional ecosystem model of the equatorial Pacific upwelling system, Part I: model development and silicon and nitrogen cycle. *Deep Sea Research II* 49, 2713-2745.
- Chavez, F., Chu, S., Elliott, S., and Maltrud, M., 2003. Observations and models of iron fertilization. *EGS-AGU-EUG Joint Assembly*, Nice, France April 6-11.
- Chu, S. and Elliott, S., 2001. Latitude versus depth simulations of ecodynamics and dissolved gas chemistry relationships in the central Pacific. *J. Atmos. Chem.* 40(3), 305-333.
- Chu, S., S. Elliott and Maltrud, M., 2003. Global eddy permitting simulations of surface ocean nitrogen, iron, sulfur cycling, *Chemosphere: Global Change Science* 50, 223-235.
- Coale, K. H. and 18 others, 1996. A massive phytoplankton bloom induced by an ecosystem scale iron fertilization experiment in the equatorial Pacific Ocean, *Nature* 383, 495-501.
- Conkright, M., O'Brien, T., Levitus, S., Boyer, T. P., Antonov, J., and Stephens, C., 1998. World Ocean Atlas 1998. Vol 10-12. Nutrient and chlorophyll of the Atlantic (Vol-10), Pacific (Vol-11), and Indian (Vol-12) Oceans. *NOAA Atlas NESDIS* 36-38. U.S. Gov. Printing Office, Wash., D. C.
- Doney, S. C., Glover, D. M., and Najjar, R. G., 1996. A new coupled, one-dimensional biological-physical model for the upper ocean: Application to the JGOFS Bermuda Atlantic Time-series Study (BATS) site, *Deep Sea Research II* 43(2-3), 591-624.
- Doney, S. C., Kleypas J. A., Sarmiento J. L. and Falkowski, P. G., 2002. The US JGOFS synthesis and modeling project – an introduction. *Deep Sea Research II* 49, 1-20.
- Dukowicz, J.K., Smith, R.D., and Malone, R.C., 1993. A reformulation and implementation of the Bryan Cox Semtner ocean model on the Connection Machine. *J. Atmos. Oceanic Technol.* 10, 195-208.
- Elliott, S., and Chu, S., 2003. Comment on ocean fertilization experiments initiate large scale phytoplankton blooms. *Geophys. Res. Lett.* 30, 10.1029/2002GL016255.
- Fasham, M. J. R., Ducklow, H. W., and McKelvie, S. M., 1990. A nitrogen-based model of plankton dynamics in the oceanic mixed layer. *J. Mar. Res.* 35, 357-394.
- Fasham, M. J. R., Sarmiento, J. L., Slater, R. D., Ducklow, H. W., and Williams, R., 1993. Ecosystem behavior at Bermuda station S and ocean weather station India: A general circulation model and observational analysis. *Global Biogeochem. Cycles* 7, 379-416.
- Fung, I. Y., Meyu, S. K., Tegen, I., Doney, S. C., John, J. G., and Bishop, J. K. B., 2000. Iron supply and demand in the upper ocean. *Global Biogeochem. Cycles* 14, 281-295.
- IPCC (Intergovernmental Panel on Climate Change) 1996. *Climate Change 1995*. Cambridge University Press.

- IPCC (Intergovernmental Panel on Climate Change) 2001. *Climate Change 2001*. Cambridge University Press.
- Johnson, K.S., Gordon, R.M., and Coale, K.H., 1997. What controls iron concentrations in the world ocean? *Mar. Chem.* 57, 137-161.
- Kettle, A. J. and 31 others, 1999. A global database of sea surface dimethylsulfide (DMS) measurements and a procedure to predict sea surface DMS as a function of latitude, longitude and month, *Global Biogeochem. Cycles* 13, 18715-18721.
- Levitus, S., Conkright, M. E., Reid, J. L., Najjar, R. G., and Mantyla, A., 1993. Distribution of nitrate, phosphate and silicate in the world oceans. *Prog. Oceanogr.* 31, 245-273.
- Longhurst, A., 1998. *Ecological Geography of the Sea*. Academic Press, New York.
- Maier-Reimer, E., 1993. Geochemical cycles in an ocean general circulation model: Preindustrial tracer distributions. *Global Biogeochem. Cycles* 7, 645-677.
- Maltrud, M. E., Smith, R., Semtner, A. J., and Malone, R. C., 1998. Global eddy resolving ocean simulations driven by 1985-1995 atmospheric winds. *J. Geophys. Res.* 103, 30825-30853.
- Martin, J. H. and 43 others, 1994. Testing the iron hypothesis in ecosystems of the equatorial Pacific Ocean, *Nature* 371, 123-129.
- McGillicuddy, D.J., Anderson, L.A., Doney, S.C., and Maltrud, M.E., 2003. Eddy driven sources and sinks of nutrients in the upper ocean: Results from an 0.1 degree resolution model of the North Atlantic. *Global Biogeochem. Cycles*, in press.
- Moore, J. K., Doney, S. C., Kleypas, J. A., Glover, D. M., and Fung, I. Y., 2002. An intermediate complexity marine ecosystem model for the global domain. *Deep Sea Research II* 49, 403-462.
- Ryabchenko, V. A., Fasham, M. J. R., Kagan, B. A., and Popova, E. E., 1997. What causes short-term oscillations in ecosystem models of the ocean mixed-layer? *J. Marine Systems* 13, 33-50.
- Sarmiento, J.L., and Orr, J.C., 1991 Three dimensional simulations of the impact of Southern Ocean nutrient depletion on atmospheric carbon dioxide and ocean chemistry, *Limnol. Oceanogr.* 36, 1928-1950.
- Sarmiento, J. L., Slater, R. D., Fasham, M. J. R., Ducklow, H. W., Toggweiler, J. R., and Evans, G. T., 1993. A seasonal three dimensional ecosystem model of nitrogen cycling in the North Atlantic euphotic zone. *Global Biogeochem. Cycles* 7, 417-450.
- Semtner, A.J. 1986. Modeling the ocean in climate studies. *Adv. Phys. Oceanogr.* 187-201.
- Smith, R.D., Maltrud, M.E., Bryan, F., and Hecht, M.W., 2000. Numerical simulation of the North Atlantic Ocean at 1/10 degree. *J. Phys. Oceanogr.* 30, 1532-1561.
- Takahashi, T. and 11 others, 2002. Global sea-air CO₂ flux based on climatological surface ocean partial pressures and seasonal biological and temperature effects. *Deep Sea Research II* 49, 1601-1622.
- Tomczak, M. and Godfrey, J. S., 1994. *Regional Oceanography*. Pergamon, Elmsford, NY.
- Watson, A.J. and Liss, P.S., 1998. Marine biological controls on climate via the carbon and sulphur geochemical cycles. *Phil. Trans. R. Soc. Lond. B* 353, 41-51.